Cell Metabolism
Short Article

PARP-1 Inhibition Increases Mitochondrial Metabolism through SIRT1 Activation

Péter Bai,[1,2] Carles Cantó,[3] Hugues Oudart,[4] Attila Brunyánszki,[2] Yana Cen,[5] Charles Thomas,[3] Hiroyasu Yamamoto,[3] Aline Huber,[1] Borbála Kiss,[1] Riekelt H. Houtkooper,[3] Kristina Schoonjans,[3] Valérie Schreiber,[1] Anthony A. Sauve,[5] Josiane Menissier-de Murcia,[1] and Johan Auwerx[3,*]
[1]Biotechnologie et Signalisation Cellulaire, UMR7242 CNRS, Université de Strasbourg, ESBS, Illkirch, France
[2]Department of Medical Chemistry, University of Debrecen, Debrecen, Hungary
[3]Laboratory of Integrative and Systems Physiology, École Polytechnique Fédérale de Lausanne, Switzerland
[4]CEPE, CNRS UPR9010, Strasbourg, France
[5]Department of Pharmacology, Weill Cornell Medical College, New York, NY 10021, USA
*Correspondence: admin.auwerx@epfl.ch
DOI 10.1016/j.cmet.2011.03.004

SUMMARY

SIRT1 regulates energy homeostasis by controlling the acetylation status and activity of a number of enzymes and transcriptional regulators. The fact that NAD^+ levels control SIRT1 activity confers a hypothetical basis for the design of new strategies to activate SIRT1 by increasing NAD^+ availability. Here we show that the deletion of the poly(ADP-ribose) polymerase-1 (*PARP-1*) gene, encoding a major NAD^+-consuming enzyme, increases NAD^+ content and SIRT1 activity in brown adipose tissue and muscle. *PARP-1*$^{-/-}$ mice phenocopied many aspects of SIRT1 activation, such as a higher mitochondrial content, increased energy expenditure, and protection against metabolic disease. Also, the pharmacologic inhibition of PARP in vitro and in vivo increased NAD^+ content and SIRT1 activity and enhanced oxidative metabolism. These data show how PARP-1 inhibition has strong metabolic implications through the modulation of SIRT1 activity, a property that could be useful in the management not only of metabolic diseases, but also of cancer.

INTRODUCTION

Intracellular NAD^+ levels control the activity of the type III deacetylase SIRT1, allowing it to act both as a metabolic sensor and effector (Yu and Auwerx, 2009). Overexpression studies indicated how activation of SIRT1 or of its orthologs extends life span in lower eukaryotes and protects against high-fat-diet (HFD)-induced metabolic disease in mice (Yu and Auwerx, 2009). These attractive properties spurred a quest to identify small-molecule SIRT1 agonists that could be used in situations of metabolic stress and damage. This strategy identified compounds like resveratrol or SRT1720 (Howitz et al., 2003; Milne et al., 2007), whose ability to directly interact with and activate SIRT1 is, however, debated (Pacholec et al., 2010). Therefore, a strong interest exists to develop alternative strategies to activate SIRT1. Given the NAD^+ dependency of SIRT1, another potential way to activate it is by increasing NAD^+ availability. This could be achieved by specifically inhibiting other NAD^+-consuming activities.

Poly(ADP-ribose) polymerase (PARP)-1 is a major cellular NAD^+ consumer (Sims et al., 1981). PARP-1 is activated upon binding to damaged or abnormal DNA (Durkacz et al., 1980) and catalyzes the formation of poly(ADP-ribose) polymers (PAR) onto different acceptor proteins, including PARP-1 itself (autoPARylation), using NAD^+ as substrate (Adamietz, 1987). PARP-1 activation depletes cellular NAD^+ levels, using it to form PAR (Sims et al., 1981). This led us to test the influence of PARP-1 on SIRT1 activity and metabolic homeostasis. Our results show how a reduction/ablation of PARP-1 activity boosts NAD^+ levels and SIRT1 activity, which in turn enhances mitochondrial content and function, culminating in a solid protection against metabolic disease.

RESULTS

PARP-1$^{-/-}$ Mice Are Leaner and Have Increased Energy Expenditure

Chow-fed *PARP-1*$^{-/-}$ mice (de Murcia et al., 1997) weighed less (Figure 1A) and accumulated less fat than *PARP-1*$^{+/+}$ littermates upon aging (Figure 1B), despite eating significantly more (Figure 1C). During indirect calorimetry, *PARP-1*$^{-/-}$ mice consumed more O_2 (Figure 1D), suggestive of higher energy expenditure (EE). Resting EE was not different (Figure S1A), indicating that the increase was due to changes at night, when mice are active. Accordingly, *PARP-1*$^{-/-}$ mice were more active at night (Figure S1B). In addition, the respiratory quotient was also higher in *PARP-1*$^{-/-}$ mice during the dark phase, indicating enhanced glucose oxidation during the feeding period (Figure 1E). *PARP-1*$^{-/-}$ mice also maintained a higher body temperature upon cold exposure (Figure 1F), were more glucose tolerant (Figure 1G), and had a trend toward lower fasting blood glucose levels (4.30 ± 0.17 mM in *PARP-1*$^{+/+}$ mice versus 3.98 ± 0.18 mM in *PARP-1*$^{-/-}$ mice; $p = 0.058$), despite similar insulin levels (data not shown). During euglycemic-hyperinsulinemic clamp, glucose infusion rates or hepatic glucose production were similar to *PARP-1*$^{+/+}$ mice,

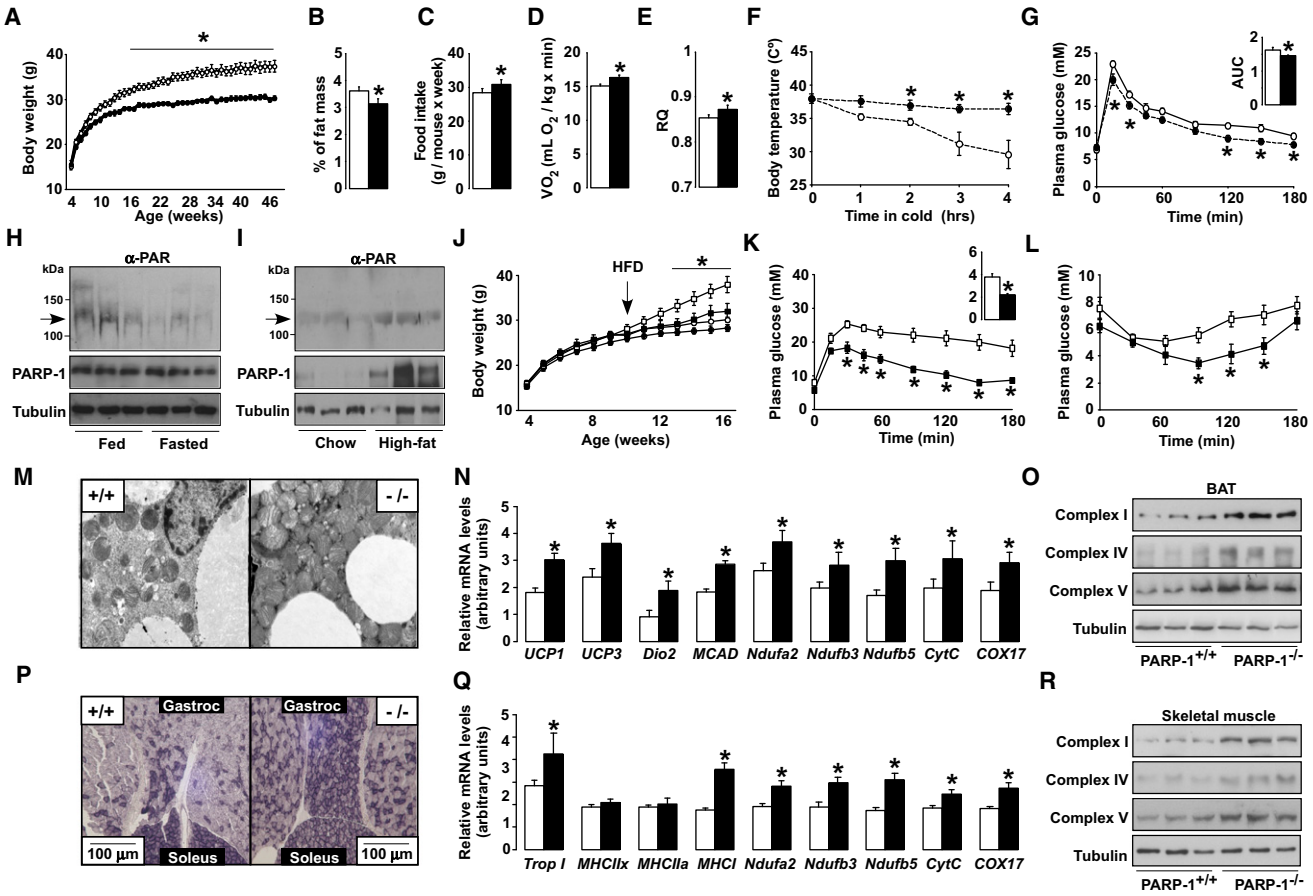

Figure 1. Phenotyping the PARP-1$^{-/-}$ Mice

(A) Body weight (BW) evolution in *PARP-1*$^{+/+}$ and $^{-/-}$ mice (n = 8/9).

(B) Epididymal white adipose tissue mass.

(C) Average food consumption.

(D and E) O_2 consumption (D) and respiratory quotient (RQ) (E) of *PARP-1*$^{+/+}$ and $^{-/-}$ mice (n = 9/9) determined by indirect calorimetry.

(F) Body temperature after exposure to 4°C (n = 6/5).

(G) Oral glucose tolerance test (OGTT) (n = 5/5) and the area under curve (AUC).

(H) PARP-1 autoPARylation (arrow), analyzed in 100 µg of protein extract from gastrocnemius muscles of 16-week-old mice fed ad libitum or fasted (24 hr). PARP-1 and tubulin levels were checked using 50 µg of protein extract.

(I) Gastrocnemius from mice on chow diet (CD) or HFD (12 weeks) were analyzed as in (H).

(J) BW evolution in *PARP-1*$^{+/+}$ and $^{-/-}$ mice (n = 10/10) fed a CD (circles) or HFD (squares) from 8 weeks of age.

(K and L) OGTT (K) and an insulin tolerance test (L) in HFD-fed *PARP-1*$^{+/+}$ and $^{-/-}$ mice at 16 weeks of age (n = 10/10). The AUC of the OGTT is shown on the top right.

(M–O) BAT from *PARP-1*$^{+/+}$ and $^{-/-}$ mice on CD was extracted and mitochondrial biogenesis was analyzed by transmission electron microscopy (M), mRNA expression of the genes indicated (N), and the abundance of mitochondrial complexes (O) in 25 µg of total protein extracts.

(P) SDH staining of sections from gastrocnemius and soleus of *PARP-1*$^{+/+}$ and $^{-/-}$ mice on CD.

(Q and R) Gastrocnemius was also used to analyze mRNA levels of the indicated genes (Q) and the abundance of mitochondrial complexes in 25 µg of total protein extracts (R). White bars represent *PARP-1*$^{+/+}$ mice; black bars represent *PARP1*$^{-/-}$ mice. Values are expressed as mean ± SEM unless otherwise stated. * indicates statistical difference versus *PARP-1*$^{+/+}$ mice at $p < 0.05$. For abbreviations, see Table S1.

but supporting the idea of their better glucose tolerance, glucose uptake in *PARP-1*$^{-/-}$ muscle trended up (Figures S1C–S1E). In line with the lower fat mass and improved glucose tolerance, serum triglycerides (1.04 ± 0.07 mM in *PARP-1*$^{+/+}$ versus 0.84 ± 0.05 mM in *PARP-1*$^{-/-}$ mice; p = 0.048) and free fatty acids (FFA) (0.93 ± 0.09 mEq/l in *PARP-1*$^{+/+}$ versus 0.72 ± 0.03 mEq/l in *PARP-1*$^{-/-}$ mice; p = 0.040) were reduced in *PARP-1*$^{-/-}$ mice.

PARP-1 Is Induced by Nutrient Availability and Contributes to HFD-Induced Diabesity

The metabolic impact of *PARP-1* deletion made us evaluate whether nutrient scarcity (fasting) or overload (HFD) affects PARP-1 activity. Despite similar PARP-1 protein levels, a 24 hr fast sharply reduced PARP-1 autoPARylation levels, which reflect global PARP activity (Adamietz, 1987), suggesting a lower enzymatic activity (Figure 1H). In contrast, HFD robustly

increased PARP-1 protein levels and activity (Figure 1I), indicating a positive correlation between PARP-1 activity and nutrient availability.

As nutrient availability induces PARP-1 activity and *PARP-1* deletion prompts a leaner phenotype, we next explored how *PARP-1*$^{-/-}$ mice responded to HFD-induced metabolic disease. *PARP-1*$^{-/-}$ mice gained less weight after 2 months of HFD (Figure 1J), due to a lower fat accumulation (Figure S1F). Moreover, *PARP-1*$^{-/-}$ mice on HFD were more glucose tolerant (Figure 1K) insulin sensitized (Figure 1L) and had lower serum FFAs (0.66 ± 0.05 mEq/l versus 0.53 ± 0.03 mEq/l; p = 0.026).

Mitochondrial Activation in Brown Adipose Tissue and Muscle from PARP-1$^{-/-}$ Mice

The above results suggested improved mitochondrial activity in key metabolic tissues of *PARP-1*$^{-/-}$ mice, such as skeletal muscle and brown adipose tissue (BAT). *PARP-1*$^{-/-}$ mice had a relatively higher amount of BAT, with a more intense red appearance (Figure S1G). Transmission electron microscopy revealed higher mitochondrial content in *PARP-1*$^{-/-}$ BAT (Figure 1M), which was further corroborated by the increased mitochondrial DNA content (Figure S1H) and mRNA expression of genes involved in mitochondrial respiration (*Ndufa2*, *Ndufb2*, *Ndufb5*, *Cyt C*, *COX17*), uncoupling (*UCP1*, *UCP3*), fatty acid oxidation (*MCAD*), and thyroid hormone activation (*Dio2*). Mitochondrial biogenesis was also evidenced by the higher protein content of subunits from different respiratory complexes in the BAT from *PARP-1*$^{-/-}$ mice (Figure 1O).

Also, *PARP-1*$^{-/-}$ skeletal muscle had a marked oxidative profile. Succinate dehydrogenase (SDH) staining (Figure 1P) and the expression of muscle fiber isotype genes (*Trop I*, *MHCI*) (Figure 1Q) exposed an increase in oxidative fibers with a high mitochondrial content. As in BAT, the increased mitochondrial content was linked to an induction of the mRNA (Figure 1Q) and protein levels (Figure 1R) of mitochondrial components. In contrast to BAT and muscle, the expression of key metabolic genes was not altered in *PARP-1*$^{-/-}$ livers (Figure S1I), reflecting a minor role of PARP-1 in the liver, probably due to its very low expression (Figure S1J).

Higher NAD$^+$ Content and SIRT1 Activity in BAT and Muscle from PARP-1$^{-/-}$ Mice

The *PARP-1*$^{-/-}$ mice phenocopy many features seen after SIRT1 activation (Yu and Auwerx, 2009). As PARP-1 is a major NAD$^+$ consumer (Sims et al., 1981), we speculated that the lack of PARP-1 activity might increase NAD$^+$ content, in turn activating SIRT1. Illustrating how PARP-1 drives most PARP activity, the ablation of *PARP-1* reduced PARylation in both BAT and muscle (Figure 2A). The expression of the other PARP enzymes was not increased in *PARP-1*$^{-/-}$ BAT and muscle (Figures S2A and S2B), explaining the lack of compensation on PARylation. Confirming previous studies (Allinson et al., 2003; Fong et al., 2009), terminal dUTP nick-end labeling indicated that DNA damage was not increased in *PARP-1*$^{-/-}$ tissues (data not shown). In line with the attenuated NAD$^+$-consuming PARP activity, NAD$^+$ content was robustly increased in *PARP-1*$^{-/-}$ BAT and muscle (Figure 2B), while the levels of nicotinamide (NAM), a NAD$^+$-derived metabolite that inhibits sirtuin activity (Bitterman et al., 2002), remained unaffected (Figure 2C).

We next tested if the increase in NAD$^+$ correlated with SIRT1 activation. Indicative of SIRT1 activation, and supporting the higher mitochondrial content, PGC-1α acetylation levels in BAT and muscle of *PARP-1*$^{-/-}$ mice were reduced by ~40% and ~90%, respectively (Figures 2D and 2E). The acetylation of another SIRT1 target, forkhead box O1 (FOXO1), was also reduced by ~60% in BAT and ~40% in muscle (Figures 2D and 2E), supporting the idea that *PARP-1* deficiency leads to SIRT1 activation. Remarkably, SIRT1 protein was also robustly induced in *PARP-1*$^{-/-}$ BAT and muscle (Figures 2D and 2E), further amplifying SIRT1 activity.

As altered NAD$^+$ levels could also potentially impact other sirtuins, we also tested the activity of SIRT2 and SIRT3, which act as cytoplasmic and mitochondrial sirtuins, respectively. The acetylation level of tubulin, a SIRT2 target (North et al., 2003), was not altered in muscle from *PARP-1*$^{-/-}$ mice (Figure 2F). Likewise, the acetylation of complex I, a target for SIRT3 (Ahn et al., 2008), even showed a slight tendency to increase in *PARP-1*$^{-/-}$ muscles (Figure 2G). These results indicate that not all sirtuins are activated in *PARP-1*$^{-/-}$ tissues.

Reduced PARP-1 Activity in Cellular Models Enhances Oxidative Metabolism

Next, we knocked down *PARP-1* in HEK293T cells to evaluate whether an acute reduction in PARP-1 activity enhances oxidative metabolism. In these conditions, PARP-1 protein levels were reduced by ~80%, and the low PARP-1 autoPARylation demonstrated that PARP activity was largely blunted (Figure 3A). The reduced PARP activity was associated with enhanced NAD$^+$ content and SIRT1 function, as illustrated by decreased PGC-1α acetylation (Figures 3B and 3C). Importantly, this happened despite unchanged SIRT1 protein levels (Figure 3C) or changes in the activity of SIRT2 or SIRT3, as manifested in tubulin, Ndufa9, or total mitochondrial acetylation levels (Figures S3A–S3C). The induction of SIRT1 and PGC-1α activity culminated in a robust increase in mitochondrial DNA content (Figure 3D), mitochondrial-related gene expression (Figure 3E), and O_2 consumption (Figure 3F). Importantly, most of the metabolic effects elicited by PARP-1 depletion were lost when SIRT1 was simultaneously knocked down (Figures 3D–3F).

In line with the results in HEK293T cells, the expression of genes involved in mitochondrial function, mitochondrial DNA content, and O_2 consumption were also induced in *PARP-1*$^{-/-}$ compared to *PARP-1*$^{+/+}$ MEFs (Figures S3D–S3F). Consistent with our observations in tissues from *PARP-1*$^{-/-}$ mice, SIRT1 protein was also induced in *PARP-1*$^{-/-}$ MEFs (Figure S3G).

Pharmacological PARP Inhibition Enhances Oxidative Metabolism via SIRT1

To test the relation between SIRT1 and PARP-1 activities, we exposed C2C12 myotubes to H_2O_2 (500 μM, 6 hr), a well-known inducer of PARP-1 activity (Schraufstatter et al., 1986). H_2O_2 treatment vigorously increased PARP-1 (Figure 4A) and global protein PARylation levels (Figure 4B), as manifested by the slow migrating bands, in the absence of changes in PARP-1 levels (Figures 4A and 4B). Importantly, SIRT1 was not PARylated in response to H_2O_2 (Figure 4A), indicating that it is not a PARylation substrate. As reported (Schraufstatter et al., 1986), the H_2O_2-induced increase in PARP-1 activity sharply

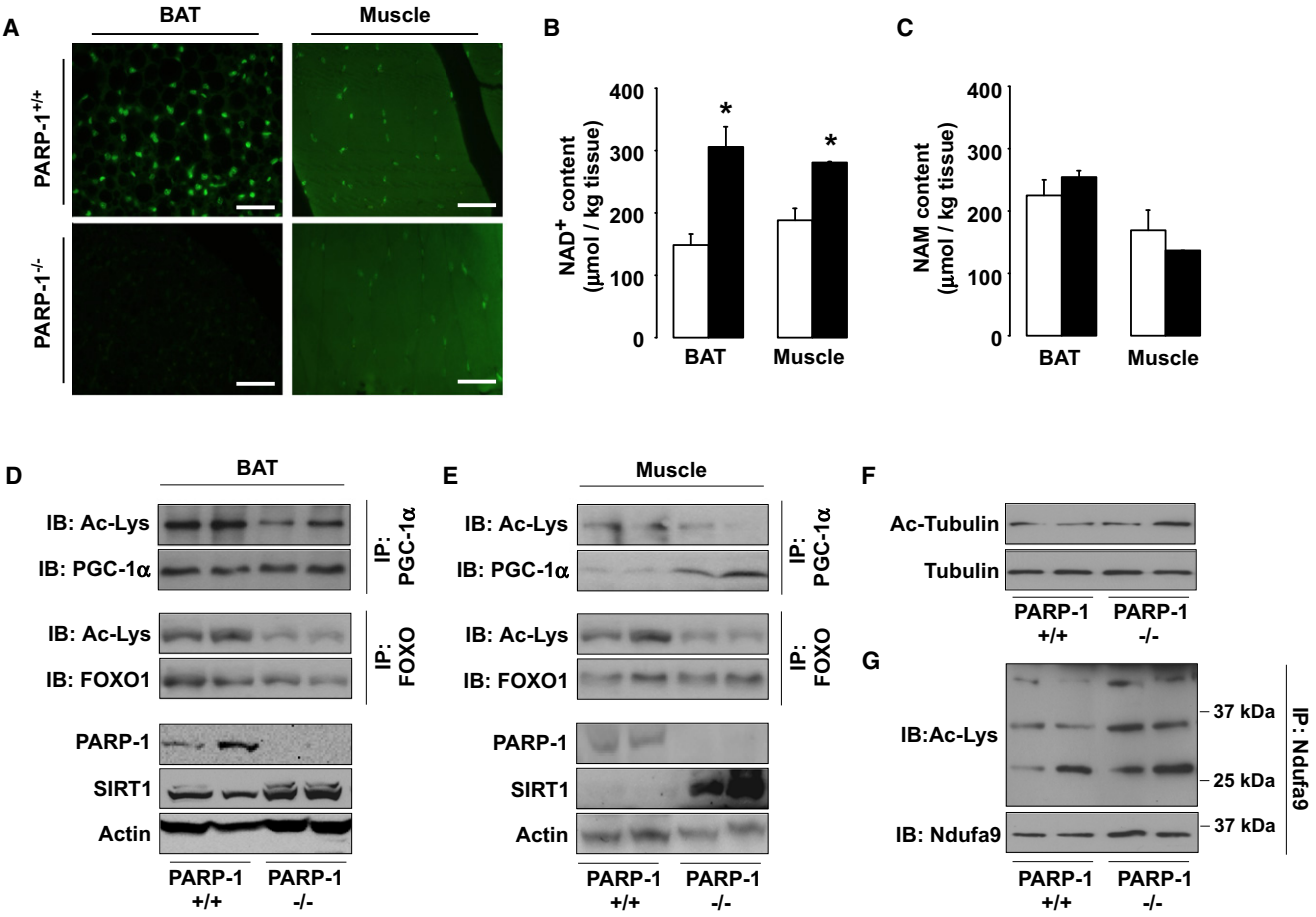

Figure 2. PARP-1 Deletion Raises NAD^+ Levels and Activates SIRT1

(A) Protein PARylation determined by α-PAR staining on formalin-fixed 7 µm BAT and muscle tissue sections of *PARP-1*$^{+/+}$ and $^{-/-}$ mice. White bar = 10 µm.

(B and C) NAD^+ (B) and NAM (C) levels in BAT and muscle from *PARP-1*$^{+/+}$ (white bars) and *PARP-1*$^{-/-}$ (black bars) mice determined by mass spectrometry.

(D and E) PARP-1, SIRT1, and actin protein content in BAT (D) and muscle (E) were determined by western blot, using 100 µg of protein lysate. PGC-1α and FOXO1 acetylation were examined by immunoprecipitation.

(F) Tubulin and acetylated-tubulin levels were tested in *PARP-1*$^{+/+}$ and $^{-/-}$ gastrocnemius.

(G) The Ndufa9 subunit of mitochondrial complex I was immunoprecipitated from 400 µg of total protein from gastrocnemius, and acetylation levels were analyzed by western blot. Values are expressed as mean ± SEM unless otherwise stated. * indicates statistical difference versus *PARP-1*$^{+/+}$ mice at $p < 0.05$.

depleted NAD^+ content (Figure 4C), but did not affect SIRT1 protein levels (Figures 4A and 4B). This lower NAD^+ availability limited SIRT1 activity, as reflected in PGC-1α hyperacetylation (Figure 4D). Interestingly, the inhibition of PARP activity with PJ34 (Garcia Soriano et al., 2001) rescued the drop in NAD^+ and recovered SIRT1 function during H_2O_2 exposure (Figures 4B–4D). These results indicate that PARP-1 activation restrains SIRT1 activity and that PARP inhibitors relieve this limitation.

PARP-1 activity is not necessarily linked to DNA damage, and it has been shown to fluctuate in a circadian fashion (Asher et al., 2010). Therefore, we wondered whether prolonged PARP inhibition, even in the absence of DNA damage, would favor NAD^+ accumulation and, potentially, SIRT1 activity. Supporting this premise, PARP inhibition by PJ34 (Figure 4E) or a structurally unrelated compound, TIQ-A (data not shown), gradually raised NAD^+ levels, becoming significant after 24 hr. At that time, PARP activity, but not PARP-1 protein levels, was robustly decreased (Figure 4F). PJ34 increased NAD^+ levels dose dependently, in correlation with SIRT1 activity, as illustrated by PGC-1α deacetylation (Figure 4G). Similar effects also happened in vivo, as treatment of mice with PJ34 (10 mg/kg, b.i.d. for 5 days) blunted basal PARP activity in muscle (Figure 4H), while increasing NAD^+ and SIRT1 activity (Figure 4I). Despite the short duration of the treatment, serum triglyceride (1.21 ± 0.08 mM vehicle versus 1.11 ± 0.04 mM PJ34; $p = 0.08$) and FFA levels (1.59 ± 0.06 mEq/l vehicle versus 1.44 ± 0.03 mEq/l PJ34; $p = 0.03$) were reduced in PJ34-treated mice. Of note, while compounds like resveratrol impact SIRT1 through AMP-activated protein kinase (AMPK) (Cantó et al., 2010), PJ34 did not alter AMPK activity, as reflected by the unchanged acetyl-CoA carboxylase (ACC) phosphorylation in either C2C12 myotubes (Figure 4J) or gastrocnemius muscle (Figure 4H). PJ34 did not affect SIRT1 protein levels either (Figures 4H and 4J), but robustly induced the expression of mitochondrial and lipid oxidation genes, both in C2C12 myotubes and muscle (Figures 4K and 4L). Consistent with PGC-1α deacetylation and activation,

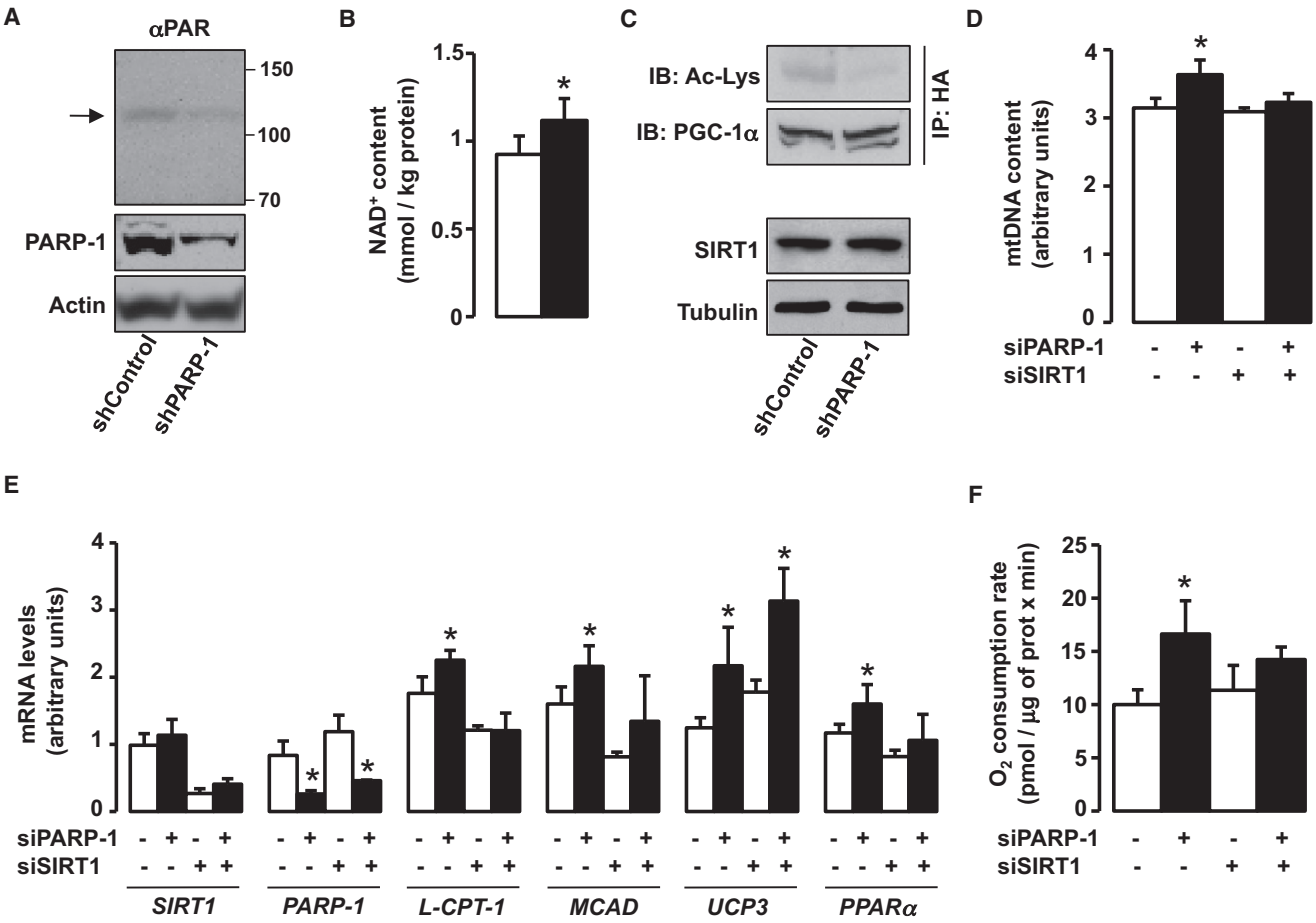

Figure 3. PARP-1 Knockdown Promotes SIRT1 Activity and Oxidative Metabolism

(A–C) HEK293T cells were transfected with either scramble (control) or *PARP-1* shRNA and HA-PGC-1α expression vector for 48 hr. Then, PARP-1 protein levels and autoPARylation (arrowhead) were analyzed in total protein lysates (A). Intracellular NAD^+ was measured on total acid extracts (B). PGC-1α acetylation was analyzed in HA immunoprecipitates (C).

(D–F) HEK293T cells were transfected with either a pool of *PARP-1* siRNAs, a pool of *SIRT1* siRNAs, or different combinations of both using the corresponding scramble siRNAs as control (−). The cells were simultaneously transfected with HA-PGC-1α for 48 hr. Then, relative mitochondrial DNA content (D), mRNA levels of the genes indicated (E), and total O_2 consumption (F) were analyzed. Values are expressed as mean ± SEM unless otherwise stated. * indicates statistical difference versus respective control sh/siRNA-transfected cells at $p < 0.05$.

PJ34 promoted the recruitment of PGC-1α to target gene promoters (e.g., PDK4) (Figure S4A). Finally, the activation of SIRT1/PGC-1α by PJ34 culminated in higher O_2 consumption rates (Figure 4M), testifying for enhanced oxidative metabolism.

The effect of PJ34 on PGC-1α acetylation in C2C12 myotubes was blunted upon *SIRT1* knockdown (Figure 4J). The role of SIRT1 in mediating PJ34-induced PGC-1α deacetylation was further confirmed in *SIRT1*$^{-/-}$ MEFs, where PJ34 was unable to decrease PGC-1α acetylation (Figure S4B). In line with impaired PGC-1α activation, mitochondrial gene expression and O_2 consumption were largely unresponsive to PJ34 upon SIRT1 depletion in C2C12 cells (Figures 4K and 4M) and in *SIRT1*$^{-/-}$ MEFs (Figures S4C and S4D), indicating that SIRT1 is a key mediator of PJ34 action. However, PJ34 also had SIRT1-independent effects, as reflected by the persistent increase in *UCP3* mRNA even after the *SIRT1* knockdown (Figure 4K). This could be explained by the fact that PJ34 does not regulate *UCP3* expression by recruitment of PGC-1α to its promoter (Figure S4A). The pharmacological inhibition of PARP recapitulates the phenotypic characteristics of the *PARP-1*$^{-/-}$ mice and reveals that these effects are largely mediated by SIRT1.

DISCUSSION

The difficulty of identifying compounds that specifically and directly bind and activate SIRT1 led us to test whether the modulation of NAD^+ availability could be an alternative path to activation of SIRT1. Our present work supports this concept by showing how the attenuation of PARP-1, another NAD^+-consuming enzyme, increases intracellular NAD^+ levels and enhances SIRT1 activity. This prompts the deacetylation and activation of key metabolic transcriptional regulators, such as PGC-1α and FOXO1, leading to increased mitochondrial content and metabolism.

Our data suggest that PARP-1 limits NAD^+ availability for SIRT1 activation. This concept originates from the differences

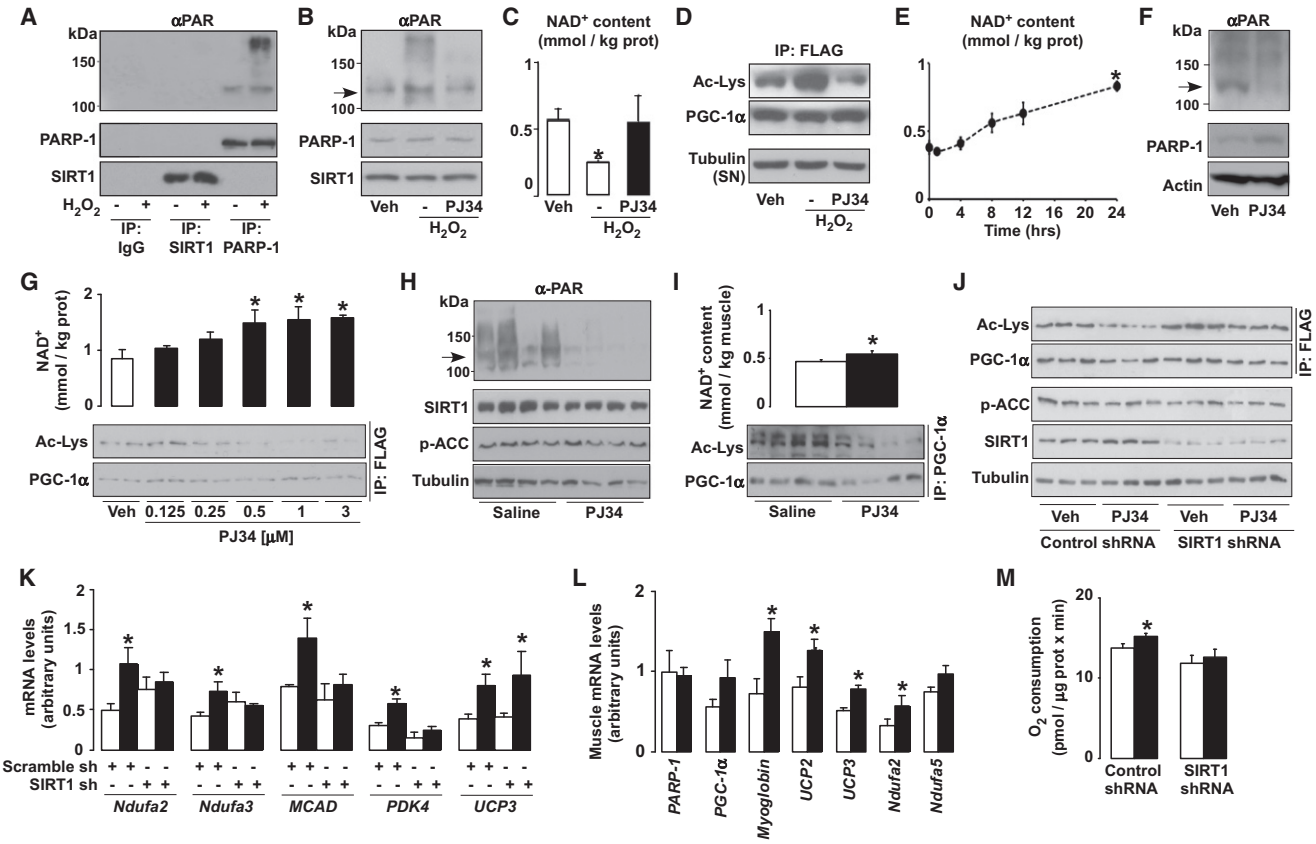

Figure 4. PARP-1 Inhibition Enhances Mitochondrial Function through SIRT1

(A–D) C2C12 myotubes expressing FLAG-HA-PGC-1α were treated for 6 hr with either PBS (vehicle [Veh]), H_2O_2 (500 μM), or H_2O_2 and PJ34 (1 μM). Then, SIRT1, PARP-1, and unspecific IgG immunoprecipitates from 500 μg of protein extracts were used to test PARylation and the proteins indicated (A). Proteins were analyzed in total cell extracts, and the arrow indicates PARP-1 autoPARylation (B). NAD^+ content was measured (C), and PGC-1α acetylation was tested in FLAG immunoprecipitates (D). Tubulin was checked on the supernatants as input.

(E) C2C12 myotubes were treated with PJ34 (1 μM) for the times indicated, and NAD^+ levels were evaluated in acidic extracts.

(F and G) C2C12 myotubes expressing FLAG-HA-PGC-1α were treated for 24 hr with PBS (Veh) or with PJ34 (1 μM, unless stated otherwise). PARP-1 protein and autoPARylation (arrow) were determined by western blot (F), and NAD^+ content and PGC-1α acetylation were measured (G).

(H and I) Ten-week-old mice received PJ34 (10 mg/kg b.i.d, i.p.) or saline (Veh) for 5 days before sacrifice (n = 10/10); then PARP-1 autoPARylation (arrow), p-ACC, and SIRT1 levels were determined in 100 μg of total protein extracts from gastrocnemius (H), and NAD^+ and PGC-1α acetylation were determined (I). PGC-1α was immunoprecipitated using 2 mg of protein from gastrocnemius muscle and 5 μg of antibody.

(J and K) C2C12 myotubes expressing FLAG-HA-PGC-1α and either a control or a SIRT1 shRNA were treated with PJ34 for 48 hr. Then, PGC-1α acetylation levels were quantified in FLAG immunoprecipitates (J), and 50 μg of total protein extracts was used to measure the other markers indicated; mRNA levels of selected genes were quantified (K).

(L) Mice were treated as in (H), and mRNA of selected genes was determined in gastrocnemius.

(M) C2C12 myotubes were treated as in (J), and cellular O_2 consumption was measured. White bars represent Veh; black bars represent PJ34 treatment. Values are expressed as mean ± SEM unless otherwise stated. * indicates statistical difference versus Veh group at $p < 0.05$. For abbreviations, see Table S1.

in the K_M and k_{cat}/K_M of both enzymes for NAD^+, which indicate that PARP-1 is a faster and more efficient NAD^+ consumer than SIRT1 (Knight and Chambers, 2001; Smith et al., 2009). Therefore, it is likely that PARP-1 activity maintains NAD^+ at limiting levels for SIRT1 function. The prediction that *PARP-1* deletion would increase NAD^+ levels and activate SIRT1 is perfectly matched by our data. While previous work already speculated on a link between PARP-1 and sirtuin activities (Kolthur-Seetharam et al., 2006; Pillai et al., 2005), our study expands the consequences of this link to energy homeostasis. In apparent discrepancy, one report (Devalaraja-Narashimha and Padanilam, 2010) suggested that *PARP-1*$^{-/-}$ mice could be more susceptible to HFD-induced obesity. However, that study used mice on an SV129 background, which are less suited for metabolic studies than C57BL/6J mice. The convergent results of our genetic, physiological, pharmacological, and in vitro studies clearly support our conclusions.

Results from our lab indicate that the activation of SIRT1 after a bout of exercise or cold exposure is not linked to decreased PARP-1 activity (data not shown). Rather, only robust and/or protracted changes, such as pharmacological (PJ34) or genetic (knockdown or deletion) PARP-1 inhibition, influence SIRT1 activity. While PARP-1 might not always participate in the physiological modulation of SIRT1 activity, our data suggest that the

interplay between both proteins could be exploited pharmacologically.

Our work illustrates the way in which SIRT1 is a key mediator of the PARP-1-deficient phenotype, but the link between PARP-1 and SIRT1 activities is still unclear. Several models used in this work show that reducing PARP-1 activity controls SIRT1 function, independent of changes in SIRT1 protein levels. In all these cases, the levels of NAD^+, the rate-limiting coenzyme for SIRT1, correlated with SIRT1 activity, suggesting that NAD^+ availability might influence SIRT1 activity. If this were true, boosting NAD^+ content through alternative strategies should elicit similar metabolic phenotypes to those of the *PARP-1*$^{-/-}$ mice. Supporting this notion, deletion of another NAD^+ consumer, CD38, also activates SIRT1 (Aksoy et al., 2006), resulting in protection against HFD-induced obesity (Barbosa et al., 2007). Nutrient scarcity and AMPK activation also lead to increased NAD^+ levels and SIRT1 activation coupled to the induction of oxidative metabolism (Cantó et al., 2009, 2010). This correlative evidence indicates that the increased NAD^+ availability might be a key mechanism by which PARP deficiency activates SIRT1. However, we cannot exclude the possibility that PARP inhibition also impacts SIRT1 via other means, even though our results rule out direct PARylation of SIRT1 as the mechanism (Figure 4A). In addition, SIRT1 content was increased in *PARP-1*$^{-/-}$ tissues and MEFs, further amplifying SIRT1 activity. The reason for this increase in SIRT1 levels remains elusive, but is independent of changes in SIRT1 mRNA (P.B., C.C., and J.A., unpublished data).

Of note, *PARP-1* depletion affects the activity of SIRT1, but not that of SIRT2 and SIRT3, which occupy nonnuclear compartments. If increased SIRT1 activity was mainly driven by changes in NAD^+, the unchanged SIRT2 and SIRT3 activities in *PARP-1*$^{-/-}$ tissues suggest that the increase in NAD^+ is either not enough to enhance SIRT2 and SIRT3 activities or that it only happens in specific cellular compartments, supporting an independent regulation of different subcellular NAD^+ pools (Yang et al., 2007). Alternatively, PARP-1 and SIRT1 activities might not be linked by changes in NAD^+, and some yet unfound mechanism drives the specificity toward this sirtuin.

Some results indicate that the effects of PARP deficiency cannot be completely explained by SIRT1 (Figure 4K). Future research will have to clarify the nature of these SIRT1-independent effects of PARP inhibition on metabolism. It will be interesting to explore whether PARylation can directly modulate the activity of key metabolic transcriptional regulators, as PARP-1 may contribute to nuclear processes other than DNA repair (Krishnakumar and Kraus, 2010).

PARP inhibitors are currently in clinical development as antitumoral drugs (Fong et al., 2009). While our data encourages a possible utilization of PARP inhibitors as therapeutic agents to activate SIRT1 and promote oxidative metabolism, this should be taken cautiously. PARP-1 has key roles in genomic maintenance, and while neither this nor previous studies (Allinson et al., 2003) detected enhanced DNA damage in *PARP-1*$^{-/-}$ mice under basal conditions, it cannot be ignored that *PARP-1*$^{-/-}$ mice are sensitive to ionizing radiation (de Murcia et al.,1997). Hence, it will be important to analyze the impact of aging and metabolic disease on DNA damage to establish the therapeutic potential and limitations of PARP inhibition.

EXPERIMENTAL PROCEDURES

Detailed materials and procedures can be found in the Supplemental Information.

Animal Experiments

Pure C57BL/6J male mice were used for the study. *PARP-1*$^{+/+}$ and *PARP-1*$^{-/-}$ were described (de Murcia et al., 1997). Mice were housed separately, had ad libitum access to water and chow (10 kcal% of fat) (SAFE, Augy, France) or HFD (60 kcal% of fat) (Research Diets, Inc., New Brunswick, NJ), and were kept in a 12 hr dark/light cycle. Animal experiments were carried out according to local, national, and EU ethical guidelines. Animals were sacrificed after 6 hr of fast, and tissues were collected and processed as specified.

NAD^+ and NAM Determination

NAD^+ levels in cultured cells were determined using an enzymatic method (EnzyChrom, BioAssays Systems, Hayward, CA), whereas for tissues (Figure 4), NAD^+ and NAM levels were determined as described (Sauve et al., 2005).

Statistics

All data were verified for normal distribution. Statistical significance was assessed by Student's t test for independent samples. Values are expressed as mean ± SEM unless otherwise stated.

SUPPLEMENTAL INFORMATION

Supplemental Information includes Supplemental Experimental Procedures, Supplemental References, four figures, and three tables and can be found with this article online at doi:10.1016/j.cmet.2011.03.004.

ACKNOWLEDGMENTS

This work was supported by fellowships awarded by Bolyai (P.B.), SNSF (P.B.), EMBO (C.C.), FEBS (A.B.), and NWO (R.H.H.), as well as grants from the NKTH, OTKA (NFF78498, IN80481), Mecenatura (DE OEC Mec-1/2008), the NIH (DK59820 and DK73466), the ERC (2008-AdG-23118), the CNRS, ANR EGIDE (22873YC), and the Ellison Medical Foundation New Scholar in Aging 2007.

Received: April 12, 2010
Revised: May 5, 2010
Accepted: February 24, 2011
Published: April 5, 2011

REFERENCES

Adamietz, P. (1987). Poly(ADP-ribose) synthase is the major endogenous nonhistone acceptor for poly(ADP-ribose) in alkylated rat hepatoma cells. Eur. J. Biochem. *169*, 365–372.

Ahn, B.H., Kim, H.S., Song, S., Lee, I.H., Liu, J., Vassilopoulos, A., Deng, C.X., and Finkel, T. (2008). A role for the mitochondrial deacetylase Sirt3 in regulating energy homeostasis. Proc. Natl. Acad. Sci. USA *105*, 14447–14452.

Aksoy, P., Escande, C., White, T.A., Thompson, M., Soares, S., Benech, J.C., and Chini, E.N. (2006). Regulation of SIRT 1 mediated NAD dependent deacetylation: a novel role for the multifunctional enzyme CD38. Biochem. Biophys. Res. Commun. *349*, 353–359.

Allinson, S.L., Dianova, I.I., and Dianov, G.L. (2003). Poly(ADP-ribose) polymerase in base excision repair: always engaged, but not essential for DNA damage processing. Acta Biochim. Pol. *50*, 169–179.

Asher, G., Reinke, H., Altmeyer, M., Gutierrez-Arcelus, M., Hottiger, M.O., and Schibler, U. (2010). Poly(ADP-ribose) polymerase 1 participates in the phase entrainment of circadian clocks to feeding. Cell *142*, 943–953.

Barbosa, M.T., Soares, S.M., Novak, C.M., Sinclair, D., Levine, J.A., Aksoy, P., and Chini, E.N. (2007). The enzyme CD38 (a NAD glycohydrolase, EC 3.2.2.5) is necessary for the development of diet-induced obesity. FASEB J. *21*, 3629–3639.

Bitterman, K.J., Anderson, R.M., Cohen, H.Y., Latorre-Esteves, M., and Sinclair, D.A. (2002). Inhibition of silencing and accelerated aging by nicotinamide, a putative negative regulator of yeast sir2 and human SIRT1. J. Biol. Chem. *277*, 45099–45107.

Cantó, C., Gerhart-Hines, Z., Feige, J.N., Lagouge, M., Noriega, L., Milne, J.C., Elliott, P.J., Puigserver, P., and Auwerx, J. (2009). AMPK regulates energy expenditure by modulating NAD+ metabolism and SIRT1 activity. Nature *458*, 1056–1060.

Cantó, C., Jiang, L.Q., Deshmukh, A.S., Mataki, C., Coste, A., Lagouge, M., Zierath, J.R., and Auwerx, J. (2010). Interdependence of AMPK and SIRT1 for metabolic adaptation to fasting and exercise in skeletal muscle. Cell Metab. *11*, 213–219.

de Murcia, J.M., Niedergang, C., Trucco, C., Ricoul, M., Dutrillaux, B., Mark, M., Oliver, F.J., Masson, M., Dierich, A., LeMeur, M., et al. (1997). Requirement of poly(ADP-ribose) polymerase in recovery from DNA damage in mice and in cells. Proc. Natl. Acad. Sci. USA *94*, 7303–7307.

Devalaraja-Narashimha, K., and Padanilam, B.J. (2010). PARP1 deficiency exacerbates diet-induced obesity in mice. J. Endocrinol. *205*, 243–252.

Durkacz, B.W., Omidiji, O., Gray, D.A., and Shall, S. (1980). (ADP-ribose)n participates in DNA excision repair. Nature *283*, 593–596.

Fong, P.C., Boss, D.S., Yap, T.A., Tutt, A., Wu, P., Mergui-Roelvink, M., Mortimer, P., Swaisland, H., Lau, A., O'Connor, M.J., et al. (2009). Inhibition of poly(ADP-ribose) polymerase in tumors from BRCA mutation carriers. N. Engl. J. Med. *361*, 123–134.

Garcia Soriano, F., Virág, L., Jagtap, P., Szabó, E., Mabley, J.G., Liaudet, L., Marton, A., Hoyt, D.G., Murthy, K.G., Salzman, A.L., Southan, G.J., and Szabó, C. (2001). Diabetic endothelial dysfunction: the role of poly(ADP-ribose) polymerase activation. Nat. Med. *7*, 108–113.

Howitz, K.T., Bitterman, K.J., Cohen, H.Y., Lamming, D.W., Lavu, S., Wood, J.G., Zipkin, R.E., Chung, P., Kisielewski, A., Zhang, L.L., et al. (2003). Small molecule activators of sirtuins extend Saccharomyces cerevisiae lifespan. Nature *425*, 191–196.

Knight, M.I., and Chambers, P.J. (2001). Production, extraction, and purification of human poly(ADP-ribose) polymerase-1 (PARP-1) with high specific activity. Protein Expr. Purif. *23*, 453–458.

Kolthur-Seetharam, U., Dantzer, F., McBurney, M.W., de Murcia, G., and Sassone-Corsi, P. (2006). Control of AIF-mediated cell death by the functional interplay of SIRT1 and PARP-1 in response to DNA damage. Cell Cycle *5*, 873–877.

Krishnakumar, R., and Kraus, W.L. (2010). The PARP side of the nucleus: molecular actions, physiological outcomes, and clinical targets. Mol. Cell *39*, 8–24.

Milne, J.C., Lambert, P.D., Schenk, S., Carney, D.P., Smith, J.J., Gagne, D.J., Jin, L., Boss, O., Perni, R.B., Vu, C.B., et al. (2007). Small molecule activators of SIRT1 as therapeutics for the treatment of type 2 diabetes. Nature *450*, 712–716.

North, B.J., Marshall, B.L., Borra, M.T., Denu, J.M., and Verdin, E. (2003). The human Sir2 ortholog, SIRT2, is an NAD+-dependent tubulin deacetylase. Mol. Cell *11*, 437–444.

Pacholec, M., Bleasdale, J.E., Chrunyk, B., Cunningham, D., Flynn, D., Garofalo, R.S., Griffith, D., Griffor, M., Loulakis, P., Pabst, B., et al. (2010). SRT1720, SRT2183, SRT1460, and resveratrol are not direct activators of SIRT1. J. Biol. Chem. *285*, 8340–8351.

Pillai, J.B., Isbatan, A., Imai, S., and Gupta, M.P. (2005). Poly(ADP-ribose) polymerase-1-dependent cardiac myocyte cell death during heart failure is mediated by NAD+ depletion and reduced Sir2alpha deacetylase activity. J. Biol. Chem. *280*, 43121–43130.

Sauve, A.A., Moir, R.D., Schramm, V.L., and Willis, I.M. (2005). Chemical activation of Sir2-dependent silencing by relief of nicotinamide inhibition. Mol. Cell *17*, 595–601.

Schraufstatter, I.U., Hinshaw, D.B., Hyslop, P.A., Spragg, R.G., and Cochrane, C.G. (1986). Oxidant injury of cells. DNA strand-breaks activate polyadenosine diphosphate-ribose polymerase and lead to depletion of nicotinamide adenine dinucleotide. J. Clin. Invest. *77*, 1312–1320.

Sims, J.L., Berger, S.J., and Berger, N.A. (1981). Effects of nicotinamide on NAD and poly(ADP-ribose) metabolism in DNA-damaged human lymphocytes. J. Supramol. Struct. Cell. Biochem. *16*, 281–288.

Smith, B.C., Hallows, W.C., and Denu, J.M. (2009). A continuous microplate assay for sirtuins and nicotinamide-producing enzymes. Anal. Biochem. *394*, 101–109.

Yang, H., Yang, T., Baur, J.A., Perez, E., Matsui, T., Carmona, J.J., Lamming, D.W., Souza-Pinto, N.C., Bohr, V.A., Rosenzweig, A., et al. (2007). Nutrient-sensitive mitochondrial NAD+ levels dictate cell survival. Cell *130*, 1095–1107.

Yu, J., and Auwerx, J. (2009). The role of sirtuins in the control of metabolic homeostasis. Ann. N Y Acad. Sci. *1173* (*Suppl 1*), E10–E19.